The MS analysis revealed that the 105 protein spots correspond to 72 distinct gene products (Fig. 1A, Supporting Information Figs. 3 and 4, Table 2, and Supporting Information Table 2). The proteins corresponding to all but five protein spots were identified by multiple peptides with significant MASCOT score (Table 2). The 68 or 37 protein spots, the intensity of which was higher or lower in the small intestinal GIST corresponded to 41 and 31 genes respectively. The protein expression level of the peptides recovered from the common preparative gels was not correlated with the MASCOT score.

3.3 Comparison between protein and mRNA expression

The intensity of the 105 identified protein spots was compared with that of the corresponding mRNA expression data generated by a DNA microarray experiment. We calculated the Spearman correlation value for the intensity of each protein spot against the mRNA expression level of their corresponding gene (Figs. 2A–D). Among the 105 protein spots examined, only 37 showed significant correlation in intensity with mRNA expression ($r > 0.449$, $p < 0.01$) (Fig. 2D). Detailed comparison between mRNA and protein expression was performed for nine gene products that generated multiple protein spots. In small intestinal GIST, all protein spots corresponding to annexin A3, glutaminase kidney isoform, and tubulin beta-2 chain showed increased intensity in 2-D DIGE, which corresponded with the mRNA expression of these genes in a statistically significant way (Fig. 2A). Both the spot intensity of 17 of 18 protein spots and mRNA expression of vimentin was higher in the small intestinal GIST (Figs. 1A and 2A, Table 2). Although all of the multiple protein spots for alpha-actinin 4, lamin A/C, pigment epithelium-derived factor and endoplasmin had different intensity between the small intestinal and gastric GIST, their mRNA expression level was not statistically different between the two groups (Fig. 2B). The mRNA expression level of vinculin was statistically higher in the small intestinal than in the gastric GIST (Fig. 2C) although two protein spots for vinculin showed increased intensity in the gastric GIST. The correlation values between the spot intensity and mRNA expression values are summarized in Table 2.

3.4 Concordance between 2-D DIGE, microarray and Western blotting data

Examination of the expression level of vimentin using Western blotting showed that it varied across the samples. Vimentin corresponded to 18 protein spots, all with statistically different intensity between the small intestinal and gastric GIST; in 17 of these spots, the intensity was higher in the small intestinal GIST (Fig. 1A and Table 2). Three bands for vimentin were observed in Western blotting (Fig. 3A). Although the higher intensity of the two bands with lower migration were specific to the small intestinal GIST, only the total intensity of all vimentin bands was taken into account in this study, as the number of samples was small. The sum of the intensity of these three bands was determined and used to compare vimentin with actin expression, actin being the internal control (Fig. 3B). The standardized expression level of vimentin was not statistically significantly different ($p = 0.0749$) between the small intestinal and gastric GIST.

4 Discussion

The anatomic site of origin affects the clinical behavior of a tumor and the molecular characteristics of GIST. Patients with gastric GIST have better prognosis than patients with intestinal GIST [4, 5], and genome-wide global studies have revealed many molecular differences between GIST arising in different sites of origin [6]. By integrating the clinical observations with the molecular aberrations associated with GIST from different sites, we will be able to further understand the molecular background of GIST and to improve the clinical modalities available to GIST patients. Unfortunately, only a limited proteomics study has been reported on GIST to date. Unfortunately, only a limited proteomics study has been reported on GIST to date. As the protein expression level cannot be fully predicted by measuring the corresponding mRNA level and proteins are a functional translation of genes, an expression study at the protein level should also be an effective strategy to establish novel biomarkers. While many lines of evidence have suggested a possible association of genotype aberrations such as exon 11 mutations with the site of origin, genotype aberrations affect the phenotypes only after they are aberrantly translated. With this notion, we performed protein expression profiling in 32 GIST cases with the aim of identifying anatomic-site specific proteins. We found 105 protein isoforms whose expression was statistically different between gastric and small intestinal GIST. This is the first report studying the proteomic signature corresponding to the anatomic site of GIST.

The overall features of the identified proteins were different between the gastric and small intestinal GIST (Figs. 1A and B). These observations suggest that these two types of GIST may have distinct molecular backgrounds, in turn explaining their differing clinical phenotypes. The acquired protein expression data should be validated using additional samples from both gastric and small intestinal GIST. As we believe that most of the identified proteins are not likely to be suitable for clinical use as biomarkers, .we focused our analysis on the proteins the expression of which showed statistically significant differences between the two groups.

We found 105 protein spots with significantly different intensity between the two GIST sample groups (Wilcoxon test p-value less than 0.01) (Fig. 1A). Among them, only 25 protein spots showed more than twofold differences. These observations may suggest two points; first, that GIST arising in different sites may share similar molecular backgrounds

Table 2. A list of identified protein

Spot no.[a]	Accession no.[b]	Identified protein[b]	Wilcoxon test *p* value	Fold difference ratio of means	*p*I (obs)[c]	*p*I[d]	MW (obs) (kDa)[c]	MW (kDa)[d]	Protein score[e]	Peptide matches	Sequence coverage (%)	Symbol	Correlation[f]	Wilcoxon test *p* value (mRNA)[g]	Fold difference ratio of means (mRNA)[g]
780	O94788	Retinal dehydrogenase 2	7.993E-04	6.639	6.0	5.9	60.8	54.8	182	4	5.4	ALDH1A2	0.677	2.652E-04	76.880
1108	P08670	Vimentin	1.925E-03	4.029	5.7	5.1	47.7	53.5	934	29	31.8	VIM	0.644	6.864E-04	1.997
862	P08670	Vimentin	5.439E-04	3.485	5.1	5.1	42.8	53.5	1349	39	54.6	VIM	0.554	6.864E-04	1.997
1022	P08670	Vimentin	1.250E-03	3.439	5.8	5.1	49.0	53.5	895	33	33.5	VIM	0.641	6.864E-04	1.997
1114	P08670	Vimentin	3.347E-03	3.006	5.7	5.1	47.7	53.5	533	13	17.0	VIM	0.615	6.864E-04	1.997
1735	P28161	Glutathione S-transferase Mu 2	1.250E-03	2.951	6.4	6.0	25.5	25.6	444	10	32.3	GSTM2	0.688	8.572E-02	1.300
1021	P08670	Vimentin	5.312E-03	2.810	5.8	5.1	49.0	53.5	789	30	27.1	VIM	0.575	6.864E-04	1.997
951	P08670	Vimentin	3.127E-04	2.801	5.9	5.1	49.7	53.5	1076	31	43.9	VIM	0.758	6.864E-04	1.997
827	P08670	Vimentin	6.443E-03	2.754	5.1	5.1	44.6	53.5	1424	63	52.3	VIM	0.582	6.864E-04	1.997
1158	P08670	Vimentin	5.312E-03	2.660	5.8	5.1	47.0	53.5	639	15	26.9	VIM	0.559	6.864E-04	1.997
854	P07237	Protein disulfide-isomerase precursor	5.031E-04	2.645	4.8	4.8	57.2	57.1	512	11	21.9	P4HB	−0.276	2.578E-01	1.080
1484	P12429	Annexin A3	1.250E-03	2.608	6.7	5.6	33.3	36.2	884	15	45.7	ANXA3	0.898	3.672E-04	2.290
851	P14625	Endoplasmin precursor	4.982E-03	2.593	4.7	4.8	57.2	92.5	274	5	6.2	TRA1	−0.065	3.145E-01	1.088
1574	P12429	Annexin A3	9.282E-04	2.587	6.5	5.6	31.2	36.2	63	1	2.8	ANXA3	−0.261	3.672E-04	2.290
544	P02768	Serum albumin precursor	1.483E-04	2.361	5.4	5.9	75.1	69.4	238	5	7.1	ALB	0.100	6.751E-01	1.182
1272	Q9Y3F4	Serine-threonine kinase receptor-associated protein	5.765E-03	2.317	5.1	5.0	45.0	38.4	250	5	15.4	STRAP	−0.096	6.905E-01	1.051
954	P08670	Vimentin	5.924E-04	2.269	6.0	5.1	49.7	53.5	508	11	21.1	VIM	0.585	6.864E-04	1.997
856	Q9NZW5	MAGUK p55 subfamily member 6	9.697E-03	2.246	5.6	5.8	57.2	61.1	205	4	7.6	MPP6	−0.015	8.572E-02	1.512
865	P08670	Vimentin	9.454E-04	2.241	5.0	5.1	42.8	53.5	805	18	32.7	VIM	0.563	6.864E-04	1.997
309	P02787	Serotransferrin precursor	4.982E-03	2.231	5.8	6.8	48.3	77.1	83	1	1.4	TF	−0.058	7.216E-01	1.036
1109	P08670	Vimentin	9.246E-03	2.204	5.7	5.1	47.7	53.5	738	16	29.2	VIM	0.592	6.864E-04	1.997
948	P08670	Vimentin	1.077E-03	2.171	5.9	5.1	49.7	53.5	866	20	34.0	VIM	0.692	6.864E-04	1.997
1506	P12429	Annexin A3	5.023E-03	2.171	6.7	5.6	32.4	36.2	1076	27	51.2	ANXA3	0.745	3.672E-04	2.290
857	P08670	Vimentin	3.518E-03	2.142	4.8	5.1	57.2	53.5	567	14	21.3	VIM	0.449	6.864E-04	1.997
1854	P00441	Superoxide dismutase [Cu-Zn]	8.213E-04	2.019	7.0	5.7	21.0	15.8	28	1	0.2	SOD1	−0.074	5.025E-01	1.073
457	Q96AY3	FK506 binding protein 10 precursor	2.487E-03	1.984	4.2	5.4	82.3	64.2	214	5	7.6	FKBP10	0.547	7.993E-04	2.336
540	O94925	Glutaminase kidney isoform, mitochondrial precursor	2.444E-04	1.968	5.5	7.9	76.9	73.5	145	3	5.1	GLS	0.418	3.828E-03	5.202
1499	P12429	Annexin A3	1.715E-03	1.964	6.5	5.6	32.1	36.2	128	2	7.5	ANXA3	0.481	3.672E-04	2.290
1043	P36955	Pigment epithelium-derived factor precursor	3.374E-04	1.955	5.7	6.0	49.3	46.3	114	2	5.0	SERPINF1	0.298	5.295E-01	1.480
1830	P28065	Proteasome subunit beta type 9 precursor	2.922E-03	1.899	6.7	4.9	22.5	23.3	130	3	11.4	PSMB9	0.751	2.632E-02	2.389
554	Q14314	Fibroleukin precursor	3.029E-03	1.864	5.3	7.1	76.9	50.2	92	2	4.1	FGL2	−0.002	5.295E-01	1.062
481	P02545	Lamin A/C	5.121E-03	1.817	5.7	6.6	82.3	74.1	1277	22	34.5	LMNA	0.193	6.448E-01	1.003
812	P00352	Retinal dehydrogenase 1	1.790E-03	1.809	5.5	6.3	57.2	54.7	320	8	11.6	ALDH1A1	0.577	2.919E-03	11.300
63	P18206	Vinculin	3.670E-03	1.805	4.1	5.5	114.1	123.7	90	2	1.5	VCL	−0.348	2.922E-03	1.770

Table 2. Continued

Spot no.[a]	Accession no.[b]	Identified protein[b]	Wilcoxon test p value	Fold difference ratio of means	p/ (obs)[c]	p/[d]	MW (obs) (kDa)[c]	MW (kDa)[d]	Protein score[e]	Peptide matches	Sequence coverage (%)	Symbol	Correlation[f]	Wilcoxon test p value (mRNA)[g]	Fold difference ratio of means (mRNA)[g]
1723	P04632	Calpain small subunit 1	1.247E-03	1.804	6.9	5.1	26.5	28.3	91	2	10.4	CAPNS1	0.224	1.021E-01	1.122
1253	P09471	Guanine nucleotide-binding protein G(o), alpha subunit 1	4.371E-03	1.799	5.8	5.3	45.0	39.9	213	4	11.6	GNAO1	0.567	1.688E-02	2.433
1194	Q13813	Spectrin alpha chain, brain	7.582E-03	1.793	4.0	5.2	90.7	284.5	178	3	1.2	SPTAN1	−0.201	4.258E-01	1.094
555	O94925	Glutaminase kidney isoform, mitochondrial precursor	7.304E-03	1.751	5.3	7.9	76.9	73.5	169	4	6.0	GLS	0.320	3.828E-03	5.202
768	P08670	Vimentin	1.670E-03	1.728	5.2	5.1	50.0	53.5	1045	29	41.7	VIM	0.360	6.864E-04	1.997
900	P68371	Tubulin beta-2 chain	1.719E-03	1.722	5.0	4.8	53.6	49.8	481	13	18.4	TUBB2	0.469	4.885E-02	1.221
977	P68363	Tubulin alpha-ubiquitous chain	2.418E-03	1.698	6.2	5.1	49.3	59.5	299	5	8.1	TUBA6	0.184	9.666E-01	1.000
551	P38646	Stress-70 protein, mitochondrial precursor	3.256E-03	1.692	5.6	5.9	46.7	73.7	1312	31	32.3	HSPA9B	−0.490	6.864E-04	1.353
55	P18206	Vinculin	7.252E-03	1.679	6.1	5.5	35.1	123.7	891	14	13	VCL	0.000	2.922E-03	1.770
771	Q9UJU6	Drebrin-like protein	8.610E-04	1.673	5.1	5.0	50.0	48.2	260	5	12.8	DBNL	0.325	7.835E-02	1.205
1361	P51858	Hepatoma-derived growth factor	2.360E-03	1.673	6.6	4.7	35.4	26.8	76	2	7.9	HDGF	0.006	9.332E-01	1.108
830	P07437	Tubulin beta-2 chain	8.828E-03	1.660	5.1	4.8	43.7	49.7	419	8	16	TUBB	0.042	1.938E-01	1.143
592	Q16555	Dihydropyrimidinase-related protein 2	3.123E-03	1.643	5.3	6.0	73.3	62.3	260	5	10.7	DPYSL2	0.486	8.278E-03	1.370
1203	P62736	Actin, aortic smooth muscle	8.382E-03	1.643	4.2	5.2	90.9	42.0	170	3	8.5	ACTA2	−0.519	2.922E-03	2.361
1689	P02743	Serum amyloid P-component precursor	7.763E-03	1.629	6.4	6.1	28.0	25.4	209	3	15.7	APCS	−0.075	1.000E+00	1.100
213	O43707	Alpha-actinin 4	3.818E-03	1.626	4.4	5.3	114.1	104.9	657	12	14.7	ACTN4	0.113	1.210E-01	1.219
552	O94925	Glutaminase kidney isoform, mitochondrial precursor	9.016E-03	1.618	5.2	7.9	76.9	73.5	190	4	6.3	GLS	0.554	3.828E-03	5.202
842	P68371	Tubulin beta-2 chain	3.667E-04	1.615	5.0	4.8	59.0	49.8	781	26	33.7	TUBB2	0.479	4.885E-02	1.221
1078	P08670	Vimentin	8.668E-03	1.615	5.8	5.1	48.3	53.5	698	16	25.4	VIM	0.555	6.864E-04	1.997
1826	P22352	Plasma glutathione peroxidase precursor	8.586E-03	1.613	6.8	8.2	22.0	25.5	119	3	14.6	GPX3	0.112	5.858E-01	1.252
765	Q02818	Nucleobindin 1 precursor	5.670E-03	1.612	5.1	5.1	50.0	53.9	441	7	15.2	NUCB1	0.050	3.350E-01	1.071
217	O43707	Alpha-actinin 4	5.662E-03	1.611	4.3	5.3	114.1	104.9	744	13	15.9	ACTN4	0.287	1.210E-01	1.219
535	O94925	Glutaminase kidney isoform, mitochondrial precursor (EC 3.5.1.2) (GLS)	2.374E-03	1.608	5.5	7.9	47.0	73.5	199	4	6.6	GLS	0.231	3.828E-03	5.202
1104	O75874	Isocitrate dehydrogenase [NADP] cytoplasmic	1.151E-04	1.607	5.8	6.5	47.7	46.7	468	10	20.5	IDH1	0.663	8.272E-03	1.392
832	P68371	Tubulin beta-2 chain	3.649E-04	1.605	4.9	4.8	59.0	49.8	729	19	36.9	TUBB2	0.470	4.885E-02	1.221
860	P14625	Endoplasmin precursor	3.847E-03	1.603	4.9	5.1	57.2	53.5	771	27	30.3	TRA1	−0.010	3.145E-01	1.088
1598	Q06323	Proteasome activator complex subunit 1	6.443E-03	1.600	4.2	5.8	89.8	28.7	260	6	23.3	PSME1	0.882	2.547E-03	2.054
918	P68371	Tubulin beta-2 chain	1.790E-03	1.598	5.0	4.8	53.6	49.8	850	21	48.3	TUBB2	0.487	4.885E-02	1.221
212	O43707	Alpha-actinin 4	7.774E-03	1.590	4.3	5.3	114.1	104.9	342	7	7.7	ACTN4	0.176	1.210E-01	1.219
488	P02545	Lamin A/C	3.347E-03	1.579	5.8	6.6	82.3	74.1	914	15	22.1	LMNA	0.254	6.448E-01	1.003
1440	P07195	L-lactate dehydrogenase B chain	2.930E-03	1.572	4.1	5.7	92.1	36.5	200	3	8.7	LDHB	0.077	1.112E-01	1.084

Table 2. Continued

Spot no.[a]	Accession no.[b]	Identified protein[b]	Wilcoxon test *p* value	Fold difference ratio of means	p*I* (obs)[c]	p*I*[d]	MW (obs) (kDa)[c]	MW (kDa)[d]	Protein score[e]	Peptide matches	Sequence coverage (%)	Symbol	Correlation[f]	Wilcoxon test *p* value (mRNA)[g]	Fold difference ratio of means (mRNA)[g]
1289	Q96C86	Scavenger mRNA decapping enzyme DcpS	1.173E-03	1.569	6.0	5.8	44.3	38.7	190	3	11.3	DCPS	0.404	5.878E-04	1.550
1388	Q15181	Inorganic pyrophosphatase	4.371E-03	1.559	4.1	5.5	92.5	32.7	78	2	6.6	PPA1	0.395	1.618E-04	2.140
655	P08670	Vimentin	9.354E-03	1.559	5.2	5.1	53.6	53.5	1206	42	41.7	VIM	0.431	6.864E-04	1.997
455	P11142	Heat shock cognate 71 kDa protein	3.080E-03	1.554	4.3	5.4	82.3	70.9	155	3	4.8	HSPA8	0.333	5.295E-01	1.024
825	P08670	Vimentin	4.982E-03	1.549	4.9	5.1	59.0	53.5	748	16	30.5	VIM	0.257	6.864E-04	1.997
1896	P09382	Galectin-1	9.222E-03	1.535	6.4	5.3	17.9	14.6	108	2	13.4	LGALS1	0.681	3.611E-02	1.326
809	Q96KP4	Cytosolic nonspecific dipeptidase	7.309E-03	1.534	5.0	5.7	43.3	52.9	70	2	4.4	CNDP2	0.033	6.516E-02	1.259
650	P31948	Stress-induced-phosphoprotein 1	7.304E-03	1.527	5.8	6.4	66.1	62.6	326	8	10.5	STIP1	–0.128	5.858E-01	1.094
352	P08238	Heat shock protein HSP 90-beta	6.620E-03	1.521	4.2	5.0	91.2	83.1	568	12	16.0	HSPCB	–0.059	6.443E-03	1.306
426	Q08493	cAMP-specific 3′,5′-cyclic phosphodiesterase 4C	2.922E-03	1.510	4.1	5.1	85.8	79.9	443	9	12.1	PDE4C	–0.193	2.947E-01	1.122
1828	P61019	Ras-related protein Rab-2A	3.579E-03	1.504	5.3	6.1	90.3	23.5	224	3	19.3	RAB2	–0.226	7.692E-01	1.044
666	P61978	Heterogeneous nuclear ribonucleoprotein K	4.215E-03	1.503	5.5	5.4	66.1	51.0	209	6	7.8	HNRPK	–0.088	9.364E-02	1.083
1604	Q9Y696	Chloride intracellular channel protein 4	1.247E-03	1.502	6.6	5.5	30.3	28.8	119	2	9.1	CLIC4	0.798	4.304E-04	1.458
1055	P31930	Ubiquinol-cytochrome-c reductase complex core protein I	2.638E-03	1.500	5.4	5.9	48.0	52.6	173	3	6.0	UQCRC1	–0.210	8.278E-03	1.384
505	P02545	Lamin A/C	6.126E-04	1.499	6.0	6.6	80.5	74.1	1363	27	33.9	LMNA	0.090	6.448E-01	1.003
1592	P35232	Prohibitin	5.858E-04	1.492	6.4	5.6	30.6	29.8	203	4	21.7	PHB	–0.226	4.982E-03	1.241
1512	P09493	Tropomyosin 1 alpha chain	6.096E-03	1.481	4.1	4.7	90.7	32.7	145	3	9.2	TPM1	0.547	5.574E-01	1.158
983	P36957	Dihydrolipoyllysine-residue succinyltransferase component	4.982E-03	1.479	6.0	9.0	49.0	48.6	203	4	9.5	GPR18	–0.165	5.574E-01	1.207
794	P08670	Vimentin	2.298E-03	1.478	5.0	5.1	50.0	53.5	1097	26	41.7	VIM	0.355	6.864E-04	1.997
1761	P60174	Triosephosphate isomerase	2.479E-03	1.463	6.9	6.5	24.5	26.5	229	4	15.3	TPI1	0.054	1.313E-01	1.289
494	P02545	Lamin A/C	2.919E-03	1.462	5.9	6.6	80.5	74.1	1508	23	32.7	LMNA	0.337	6.448E-01	1.003
1460	P40925	Malate dehydrogenase, cytoplasmic (EC 1.1.1.37)	7.720E-03	1.459	5.6	6.9	91.6	36.3	67	1	3	MDH1	0.241	9.360E-03	1.324
567	P08107	Heat shock 70 kDa protein 1	4.760E-03	1.439	5.6	5.5	46.0	70.1	1284	29	30.6	HSPA1A	0.507	2.406E-01	1.088
686	P50990	T-complex protein 1, theta subunit	2.935E-03	1.425	5.7	5.4	45.0	59.5	313	6	11.3	TCP1	0.216	7.692E-01	1.049
752	P48643	T-complex protein 1	4.494E-03	1.414	5.6	5.5	62.5	59.7	315	6	10.4	CCT5	–0.028	7.060E-01	1.079
1263	P00738	Haptoglobin precursor	6.932E-03	1.405	5.4	6.1	45.0	45.2	91	2	4.7	HP	–0.083	1.366E-01	1.702
1057	P36955	Pigment epithelium-derived factor precursor	9.013E-03	1.403	5.9	6.0	48.3	46.3	167	3	7.7	SERPINF1	0.322	5.295E-01	1.480
1510	P60900	Proteasome subunit alpha type 6	4.779E-03	1.388	5.6	6.3	91.2	27.4	74	1	5.3	PSMA6	0.491	1.913E-04	2.227
1555	P08758	Annexin A5	7.576E-03	1.374	6.1	4.9	31.5	35.8	96	2	5.3	ANXA5	–0.009	7.150E-02	1.161
730	P30153	Serine/threonine protein phosphatase 2A	6.113E-03	1.342	5.0	5.0	64.3	65.1	299	6	11.4	PPP2R1A	0.322	8.572E-02	1.226
1564	Q13011	Delta3,5-delta2,4-dienoyl-CoA isomerase	6.986E-03	1.341	6.4	6.6	31.5	36.0	86	2	5.8	ECH1	0.179	7.993E-04	1.606
1096	P61163	Alpha-centractin	8.661E-03	1.340	5.7	6.2	48.0	42.6	204	4	8.5	ACTR1A	–0.024	1.541E-01	1.179
497	P02545	Lamin A/C	7.441E-03	1.336	5.9	6.6	78.7	74.1	1492	28	36.0	LMNA	0.093	6.448E-01	1.003

Table 2. Continued

Spot no.[a]	Accession no.[b]	Identified protein[b]	Wilcoxon test *p* value	Fold difference ratio of means	p*I* (obs)[c]	p*I*[d]	MW (obs) (kDa)[c]	MW (kDa)[d]	Protein score[e]	Peptide matches	Sequence coverage (%)	Symbol	Correlation[f]	Wilcoxon test *p* value (mRNA)[g]	Fold difference ratio of means (mRNA)[g]
1559	P06753	Tropomyosin alpha 3 chain	6.859E-03	1.320	6.7	4.7	31.5	32.8	167	3	11.6	TPM3	0.393	7.692E-01	1.093
1565	Q96GD0	Pyridoxal phosphate phosphatase	8.278E-03	1.316	5.5	6.1	90.3	31.7	201	4	17.2	PDXP	−0.047	1.313E-01	1.322
1153	Q9BT78	COP9 signalosome complex subunit 4	4.364E-03	1.292	5.7	5.6	47.0	46.3	276	5	8.9	COPS4	0.157	1.000E+00	1.013
1807	Q06830	Peroxiredoxin 1	8.767E-03	1.239	5.0	8.3	92.1	22.1	80	2	9.5	PRDX1	−0.195	3.334E-05	2.010
1849	P32119	Peroxiredoxin 2	5.797E-03	1.218	6.4	5.7	21.5	21.8	96	2	9.6	PRDX2	−0.129	5.295E-01	1.112
237	P13639	Elongation factor 2	8.272E-03	1.216	4.7	6.4	114.1	95.2	200	4	4.2	EEF2	0.511	1.424E-01	1.194
1816	P30048	Thioredoxin-dependent peroxide reductase	9.202E-03	1.209	6.1	7.7	23.0	27.7	165	3	14.5	PRDX3	−0.121	3.145E-01	1.086

a) Spot numbers refer to those in Fig. 1A and Supporting Information Fig. 1.
b) Accession numbers of proteins were derived from Swiss-Prot and NCBI nonredundant databases.
c) Observed isoelectric point and molecular weight calculated according to location on the 2-D gel.
d) Theoretical isoelectric point and molecular weight obtained from Swiss-Prot and the ExPASy database (http://au.expasy.org).
e) MASCOT score for the identified proteins based on the peptide ions score ($p < 0.05$) (http://www.matrixscience.com).
f) Spearman's correlation.
g) Wilcoxon test.

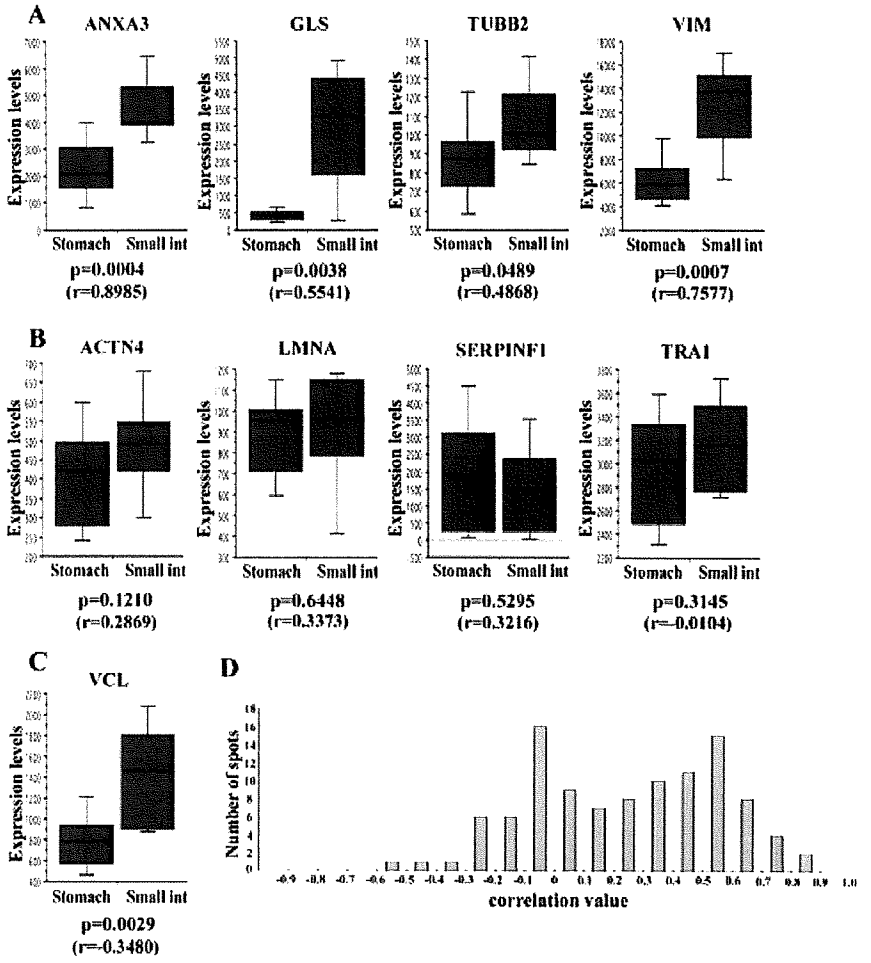

Figure 2. (A-C) A detailed comparison between mRNA and protein level is demonstrated for nine gene products that generated multiple protein spots. (A) The mRNA expression levels of annexin A3, glutaminase kidney isoform, tubulin beta-2 chain and vimentin. These genes showed different expression at the mRNA level between the gastric and small intestinal GIST (p <0.01). (B) The mRNA expression levels of alpha-actinin 4, lamin A/C, pigment epithelium-derived factor, and endoplasmin were not significantly different between the gastric and small intestinal GIST (p >0.01). (C) The mRNA expression level of vinculin. Vinculin showed significantly increased expression in the small intestinal GIST at the mRNA level (p <0.01), while vinculin expression was significantly lower in the small intestine (p <0.01). The correlation between mRNA and protein level of these genes is demonstrated by the r-value shown under the panels. (D) Among the 105 protein spots examined, only 37 showed significant correlation in intensity with mRNA expression (r >0.449, p <0.01).

at the protein level and only a limited number of proteins may have a key role in the tumors exhibiting varying clinical behavior. Indeed, the overall features of the proteome were not distinct between the intestinal and gastric tumors (Supporting Information Fig. 1). Secondly, as indicated by the number of protein spots observed in this study, 2-D DIGE uncovers only a limited portion of the proteome, which includes the proteins that are different between the two GIST types, and further improvement of the performance of 2-D DIGE will result in the identification of proteins with larger fold differences between the groups and lower expression levels.

Among the proteins identified by mass spectrometry (Fig. 1A), we found that the expression of several proteins known to be crucial to cancer development correlated with the anatomical site. One of the protein spots corresponding to prohibitin showed decreased intensity in intestinal GIST. Prohibitin has an antiproliferative activity by inhibiting DNA synthesis [16], and is down-regulated in stomach cancer [17, 18]. Similarly, the intensity of two protein spots corresponding to the pigment epithelium-derived factor (PEDF) was lower in the intestinal GIST. PEDF is neurotrophic[19] and has multifunctional antitumor activity by inhibiting the growth of tumor cells and angiogenesis[20–22]. The lower levels of PEDF have been associated with significantly poorer clinical outcome in lung cancer [23], breast cancer [24], pancreatic cancer [25], and lymphangioma [26]. These reports and our observations suggest that the decreased expression of PEDF may be associated with poor prognosis in small intestinal GIST. PEDF has been considered as a therapeutic tool in preclinical studies of ovarian cancer [27], pancreatic cancer [28], osteosarcoma [29, 30], neuroblastoma [31], melanoma [32], and liver cancer [33], suggesting that it may be similarly applied to GIST. The intensity of three alpha actinin-4 spots increased in the intestinal GIST. Alpha actinin-4 plays a key role in tumor invasion and cell motility, and aberrant expression of alpha-actinin 4 has been reported in a variety of malignancies, including prostate [34], esophageal [35], colorectal [36], lung [37, 38] and breast cancer [39]. Therefore, our proteomic study revealed a novel association

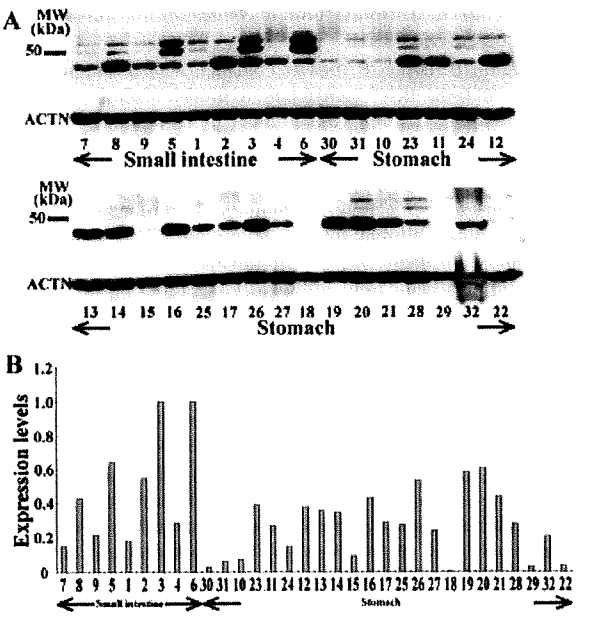

Figure 3. Western blotting for vimentin. (A) Vimentin expression was monitored by Western blotting. The upper and lower panels indicate the signals for vimentin and actin, respectively. (B) The whole intensity was measured and plotted in bar graph. Expression level was calculated by standardizing a sum of the intensity of multiple vimentin bands by the intensity of actin bands of the identical membrane.

of a number of genes, previously reported to be aberrantly expressed in a range of other malignancies, with small intestinal GIST. These observations indicate that the propensity of small intestinal GIST to exhibit malignant behavior may be attributable to the general, rather than tumor-type specific, mechanisms leading to malignant behavior of tumor cells. Subsequent studies that will examine the direct correlation between the identified proteins and survival may clarify their prognostic value. Biological validation of the contribution of these proteins to the poor prognosis of patients with the small intestinal GIST will also be worth considering, using cell lines and animal models.

In our sample set, the frequency of c-kit mutations at exons 9 and 11 was significantly high in the small intestinal and gastric GIST, respectively (Table 1). A correlation between the type of c-kit mutations and the anatomical site has also been reported in previous studies [8, 40]. Therefore, the proteomic differences observed between gastric and small intestinal GIST may include differences that are due to genotype differences. As the presence of c-kit mutations is one of the major prognostic factors for GIST cases, the molecular mechanisms underlying the differences in the behavior of GIST subtypes associated with the type of KIT mutations present is of significant interest.

We observed a significant level of discordance between the spot intensity in 2-D DIGE and the mRNA level as detected using a DNA microarray (Fig. 2). This discordance, when present, does not necessarily mean that the actual expression of identical genes at the mRNA and protein level is discordant. The intensity of each spot represents the expression level of a single isoform, and a sum of the intensity values of individual spots for a certain gene presumably represents the total amount of the expressed protein. In this study, the protein spots the intensity of which was not statistically different between the gastric and small intestinal GIST were not subjected to mass spectrometric protein identification, and there may be protein spots corresponding to isoforms other than the ones identified. The fact that the mRNA and protein expression levels were not consistently concordant may be partially due to the presence of such isoforms. The discrepancy between the 2-D DIGE and Western blotting results may also be attributable to the presence of protein spots whose intensity was unchanged or inversely changed between the two sample groups. Each isoform should have a distinct function, and only one of the isoforms may be a biomarker candidate. The 2-D DIGE is a technology with superior resolution separation that allows the identification of a change of even a small population of proteins, a attribute not shared by the other conventional separation methods. However, this high resolution may at the same time limit the application for biomarker identification. We found that 18 of the 105 identified protein spots corresponded to vimentin, and 17 of 18 showed higher intensity in the small intestinal GIST samples. However, the total amount of vimentin, as measured by Western blotting, did not show significant differences between the gastric and small intestinal GIST. Furthermore, we found two bands with slower migration in the small intestinal GIST samples; as they were specific to this group, their expression is worth being examined in additional samples. These results may suggest that specific probes against specific isoform spots or bands will be required to examine the isoforms identified by 2-D DIGE using routine clinical techniques such as ELISA and immunohistochemistry. Alternatively, we may be able to construct an easy to operate, automatic, robust, cost-effective electrophoresis and western blotting device. Both approaches will be a major challenge as a next step for biomarker development by 2-D DIGE. Although GIST are the most common primary mesenchymal tumors of the digestive tract, their prevalence is limited to 15–20 *per* 1 000 000 [1, 2], limiting the number of GIST samples available for proteomic studies. Further validation studies using an adequate number of samples will need to be performed, through the collaboration between multiple institutes, to clarify the prognostic utility or otherwise of the identified proteins. We consider that the clinical application of biomarkers identified by proteomics will need to rely on the use of practical tools such as ELISA and immunohistochemistry rather than 2-D DIGE.

In this study, we did not observe gene products previously reported to be associated with GIST such as c-kit and connexin 43 [8], a fact that possibly suggests that the sensitivity of 2-D DIGE technology should be further improved in

order to comprehensively understand the proteomic aberrations of malignant tumors. We have developed an easily operated large format electrophoresis apparatus that generates 5000 protein spots, and the application of laser microdissection for accurate sampling, as well as an effective in-gel digestion protocol for protein identification [41, 42]. Continuing efforts for increasingly more comprehensive proteomics will further our understanding of cancer biology, identify crucial proteins for diagnosis and therapy, and finally benefit cancer patients.

This study was supported by the Program for Promotion of Fundamental Studies in Health Sciences of the National Institute of Biomedical Innovation of Japan, a grant-in-aid for the Third-Term Comprehensive 10-year Strategy for Cancer Control from the Ministry of Health, Labor and Wealth of Japan and a grant-in-aid for Young Scientists (start-up) No. 20890218 from the Japan Society for the Promotion of Science.

The authors have declared no conflict of interest.

5 References

[1] Joensuu, H., Kindblom, L. G., Gastrointestinal stromal tumors–a review. *Acta Orthop. Scand. Suppl.* 2004, *75*, 62–71.

[2] Miettinen, M., El-Rifai, W., L, H. L. S., Lasota, J., Evaluation of malignancy and prognosis of gastrointestinal stromal tumors: a review. *Hum. Pathol.* 2002, *33*, 478–483.

[3] Suehara, Y., Kondo, T., Seki, K., Shibata, T. *et al.*, Pfetin as a prognostic biomarker of gastrointestinal stromal tumors revealed by proteomics. *Clin. Cancer Res.* 2008, *14*, 1707–1717.

[4] Emory, T. S., Sobin, L. H., Lukes, L., Lee, D. H., O'Leary, T. J., Prognosis of gastrointestinal smooth-muscle (stromal) tumors: dependence on anatomic site. *Am. J. Surg. Pathol.* 1999, *23*, 82–87.

[5] Fletcher, C. D., Berman, J. J., Corless, C., Gorstein, F. *et al.*, Diagnosis of gastrointestinal stromal tumors: a consensus approach. *Int. J. Surg. Pathol.* 2002, *10*, 81–89.

[6] Wozniak, A., Sciot, R., Guillou, L., Pauwels, P. *et al.*, Array CGH analysis in primary gastrointestinal stromal tumors: cytogenetic profile correlates with anatomic site and tumor aggressiveness, irrespective of mutational status. *Genes Chromosomes Cancer* 2007, *46*, 261–276.

[7] Antonescu, C. R., Viale, A., Sarran, L., Tschernyavsky, S. J. *et al.*, Gene expression in gastrointestinal stromal tumors is distinguished by KIT genotype and anatomic site. *Clin. Cancer Res.* 2004, *10*, 3282–3290.

[8] Nishitani, A., Hirota, S., Nishida, T., Isozaki, K. *et al.*, Differential expression of connexin 43 in gastrointestinal stromal tumours of gastric and small intestinal origin. *J. Pathol.* 2005, *206*, 377–382.

[9] Agaram, N., Wong, G., Guo, T., Maki, R. *et al.*, Novel V600E BRAF mutations in imatinib-naive and imatinib-resistant gastrointestinal stromal tumors. *Genes Chromosomes Cancer* 2008, *47*, 853–859.

[10] Braconi, C., Bracci, R., Bearzi, I., Bianchi, F. *et al.*, Insulin-like growth factor (IGF) 1 and 2 help to predict disease outcome in GIST patients. *Ann. Oncol.* 2008, *19*, 1293–1298.

[11] Stankey RH, L. A., *Pathology and Genetics of Tumours of the Digestive System*, IARC Press, Lyon 2000.

[12] Hasegawa, T., Matsuno, Y., Shimoda, T., Hirohashi, S., Gastrointestinal stromal tumor: consistent CD117 immunostaining for diagnosis, and prognostic classification based on tumor size and MIB-1 grade. *Hum. Pathol.* 2002, *33*, 669–676.

[13] Antonescu, C. R., Sommer, G., Sarran, L., Tschernyavsky, S. J. *et al.*, Association of KIT exon 9 mutations with nongastric primary site and aggressive behavior: KIT mutation analysis and clinical correlates of 120 gastrointestinal stromal tumors. *Clin. Cancer Res.* 2003, *9*, 3329–3337.

[14] Lasota, J., Jasinski, M., Sarlomo-Rikala, M., Miettinen, M., Mutations in exon 11 of c-Kit occur preferentially in malignant versus benign gastrointestinal stromal tumors and do not occur in leiomyomas or leiomyosarcomas. *Am. J. Pathol.* 1999, *154*, 53–60.

[15] Lasota, J., Dansonka-Mieszkowska, A., Stachura, T., Schneider-Stock, R. *et al.*, Gastrointestinal stromal tumors with internal tandem duplications in 3′ end of KIT juxtamembrane domain occur predominantly in stomach and generally seem to have a favorable course. *Mod. Pathol.* 2003, *16*, 1257–1264.

[16] Nuell, M. J., Stewart, D. A., Walker, L., Friedman, V. *et al.*, Prohibitin, an evolutionarily conserved intracellular protein that blocks DNA synthesis in normal fibroblasts and HeLa cells. *Mol. Cell. Biol.* 1991, *11*, 1372–1381.

[17] Jang, J. S., Cho, H. Y., Lee, Y. J., Ha, W. S., Kim, H. W., The differential proteome profile of stomach cancer: identification of the biomarker candidates. *Oncol. Res.* 2004, *14*, 491–499.

[18] He, Q. Y., Cheung, Y. H., Leung, S. Y., Yuen, S. T. *et al.*, Diverse proteomic alterations in gastric adenocarcinoma. *Proteomics* 2004, *4*, 3276–3287.

[19] Steele, F. R., Chader, G. J., Johnson, L. V., Tombran-Tink, J., Pigment epithelium-derived factor: neurotrophic activity and identification as a member of the serine protease inhibitor gene family. *Proc. Natl. Acad. Sci. USA* 1993, *90*, 1526–1530.

[20] Dawson, D. W., Volpert, O. V., Gillis, P., Crawford, S. E. *et al.*, Pigment epithelium-derived factor: a potent inhibitor of angiogenesis. *Science* 1999, *285*, 245–248.

[21] Maik-Rachline, G , Shaltiel, S., Seger, R., Extracellular phosphorylation converts pigment epithelium-derived factor from a neurotrophic to an antiangiogenic factor. *Blood* 2005, *105*, 670–678.

[22] Doll, J. A., Stellmach, V. M., Bouck, N. P., Bergh, A. R. *et al.*, Pigment epithelium-derived factor regulates the vasculature and mass of the prostate and pancreas. *Nat. Med.* 2003, *9*, 774–780.

[23] Zhang, L., Chen, J., Ke, Y., Mansel, R. E., Jiang, W. G., Expression of pigment epithelial derived factor is reduced in non-small cell lung cancer and is linked to clinical outcome. *Int. J. Mol. Med.* 2006, *17*, 937–944.

[24] Cai, J., Parr, C., Watkins, G., Jiang, W. G., Boulton, M., Decreased pigment epithelium-derived factor expression in

human breast cancer progression. *Clin. Cancer Res.* 2006, *12*, 3510–3517.

[25] Uehara, H., Miyamoto, M., Kato, K., Ebihara, Y. *et al.*, Expression of pigment epithelium-derived factor decreases liver metastasis and correlates with favorable prognosis for patients with ductal pancreatic adenocarcinoma. *Cancer Res.* 2004, *64*, 3533–3537.

[26] Sidle, D. M., Maddalozzo, J., Meier, J. D., Cornwell, M. *et al.*, Altered pigment epithelium-derived factor and vascular endothelial growth factor levels in lymphangioma pathogenesis and clinical recurrence. *Arch. Otolaryngol. Head Neck Surg.* 2005, *131*, 990–995.

[27] Cheung, L. W., Au, S. C., Cheung, A. N., Ngan, H. Y. *et al.*, Pigment epithelium-derived factor is estrogen sensitive and inhibits the growth of human ovarian cancer and ovarian surface epithelial cells. *Endocrinology* 2006, *147*, 4179–4191.

[28] Hase, R., Miyamoto, M., Uehara, H., Kadoya, M. *et al.*, Pigment epithelium-derived factor gene therapy inhibits human pancreatic cancer in mice. *Clin. Cancer Res.* 2005, *11*, 8737–8744.

[29] Ek, E. T., Dass, C. R., Contreras, K. G., Choong, P. F.,Pigment epithelium-derived factor overexpression inhibits orthotopic osteosarcoma growth, angiogenesis and metastasis. *Cancer Gene Ther.* 2007.

[30] Ek, E. T., Dass, C. R., Contreras, K. G., Choong, P. F., Inhibition of orthotopic osteosarcoma growth and metastasis by multitargeted antitumor activities of pigment epithelium-derived factor. *Clin. Exp. Metastasis* 2007, *24*, 93–106.

[31] Streck, C. J., Zhang, Y., Zhou, J., Ng, C. *et al.*, Adeno-associated virus vector-mediated delivery of pigment epithelium-derived factor restricts neuroblastoma angiogenesis and growth. *J. Pediatr. Surg.* 2005, *40*, 236–243.

[32] Garcia, M., Fernandez-Garcia, N. I., Rivas, V., Carretero, M. *et al.*, Inhibition of xenografted human melanoma growth and prevention of metastasis development by dual antiangiogenic/antitumor activities of pigment epithelium-derived factor. *Cancer Res.* 2004, *64*, 5632–5642.

[33] Matsumoto, K., Ishikawa, H., Nishimura, D., Hamasaki, K. *et al.*, Antiangiogenic property of pigment epithelium-derived factor in hepatocellular carcinoma. *Hepatology* 2004, *40*, 252–259.

[34] Hara, T., Honda, K., Shitashige, M., Ono, M. *et al.*, Mass spectrometry analysis of the native protein complex containing actinin-4 in prostate cancer cells. *Mol. Cell. Proteomics* 2007, *6*, 479–491.

[35] Hatakeyama, H., Kondo, T., Fujii, K., Nakanishi, Y. *et al.*, Protein clusters associated with carcinogenesis, histological differentiation and nodal metastasis in esophageal cancer. *Proteomics* 2006, *6*, 6300–6316.

[36] Honda, K., Yamada, T., Hayashida, Y., Idogawa, M. *et al.*, Actinin-4 increases cell motility and promotes lymph node metastasis of colorectal cancer. *Gastroenterology* 2005, *128*, 51–62.

[37] Yamagata, N., Shyr, Y., Yanagisawa, K., Edgerton, M. *et al.*, A training-testing approach to the molecular classification of resected non-small cell lung cancer. *Clin. Cancer Res.* 2003, *9*, 4695–4704.

[38] Menez, J., Le Maux Chansac, B., Dorothee, G., Vergnon, I. *et al.*, Mutant alpha-actinin-4 promotes tumorigenicity and regulates cell motility of a human lung carcinoma. *Oncogene* 2004, *23*, 2630–2639.

[39] Honda, K., Yamada, T., Endo, R., Ino, Y. *et al.*, Actinin-4, a novel actin-bundling protein associated with cell motility and cancer invasion. *J. Cell. Biol.* 1998, *140*, 1383–1393.

[40] Corless, C. L., Fletcher, J. A., Heinrich, M. C., Biology of gastrointestinal stromal tumors. *J. Clin. Oncol.* 2004, *22*, 3813–3825.

[41] Kondo, T., Seike, M., Mori, Y., Fujii, K. *et al.*, Application of sensitive fluorescent dyes in linkage of laser microdissection and two-dimensional gel electrophoresis as a cancer proteomic study tool. *Proteomics* 2003, *3*, 1758–1766.

[42] Kondo, T., Hirohashi, S., Application of highly sensitive fluorescent dyes (CyDye DIGE Fluor saturation dyes) to laser microdissection and two-dimensional difference gel electrophoresis (2-D DIGE) for cancer proteomics. *Nat. Protoc.* 2007, *1*, 2940–2956.

RESEARCH ARTICLE

GST-P1 as a histological biomarker of synovial sarcoma revealed by proteomics

Yoshiyuki Suehara[1, 2, 3], Kazutaka Kikuta[1, 3, 4], Robert Nakayama[4, 5], Naobumi Tochigi[6], Kunihiko Seki[6], Hitoshi Ichikawa[5], Kiyonaga Fujii[1]**, Tadashi Hasegawa[6]***, Tadakazu Shimoda[6], Hisashi Kurosawa[2], Hirokazu Chuman[3], Yasuo Beppu[3], Akira Kawai[3], Setsuo Hirohashi[1] and Tadashi Kondo[1]*

[1] Proteome Bioinformatics Project, National Cancer Center Research Institute, Tokyo, Japan
[2] Department of Orthopedic Surgery, Juntendo University School of Medicine, Juntendo, Japan
[3] Orthopedic Surgery Division, National Cancer Center Hospital, Tokyo, Japan
[4] Department of Orthopedic Surgery, Keio University, Keio, Japan
[5] Cancer Transcriptome Project, National Cancer Center Research Institute, Tokyo, Japan
[6] Pathology Division, National Cancer Center Research Institute, Tokyo, Japan
[7] Clinical Laboratory Division, National Cancer Center Hospital, Tokyo, Japan

Received: October 18, 2008
Revised: November 29, 2008
Accepted: December 2, 2008

Synovial sarcoma have two histological subtypes, biphasic and monophasic, defined respectively by the presence or absence of glandular epithelial differentiation. To develop histological biomarkers for synovial sarcoma subtypes, we examined the proteomic profile using two-dimensional difference gel electrophoresis. We identified 29 protein spots whose intensity was statistically different between the monophasic (15 cases) and biphasic (9 cases) subtypes ($p < 0.01$). Mass spectrometric protein identification demonstrated that these 29 spots corresponded to 24 distinct gene products involved in cytoskeletal organization, transcription/translation, protein/collagen binding, and ion transport, as well as structural constituents of the epidermis. Two of the 29 spots derived from glutathione S-transferase P (GST-P1) had higher intensity in biphasic type. Immunohistochemistry on additional 42 synovial sarcoma cases revealed that positive expression of GST-P1 was observed in 10 of 12 biphasic (83.3%), in 4 of 27 monophasic (14.8%) and in 1 of 3 poorly differentiated synovial sarcomas ($p = 0.0002$). Among the clinico-pathological parameters examined, GST-P1 expression significantly correlated only with the histological subtype. GST-P1 had more discriminative power than the status of fusion genes SYT-SSX1 and SYT-SSX2, previously reported to be correlated with the histological subtype. These results establish GST-P1 as a histological biomarker candidate for synovial sarcoma differentiation into subtypes.

Keywords:
2-D DIGE / GST-P1 / Proteomics / Synovial sarcoma

1 Introduction

Synovial sarcoma accounts for 5–10% of soft tissue sarcomas and is primarily located in the extremities, most frequently affecting young adults. At present, the 5-year survival rate for synovial sarcoma patients is approximately 60% [1–4]. Histologically, there are two major morphological forms of synovial sarcoma; the biphasic subtype, composed of epithelial and spindle tumor cells, and the monophasic subtype, composed solely of spindle tumor cells [1]. The molecular

Correspondence: Dr. Tadashi Kondo, Proteome Bioinformatics Project, National Cancer Center Research Institute, 5-1-1 Tsukiji, Chuo-ku, Tokyo 104-0045, Japan
E-mail: takondo@ncc.go.jp
Fax: +81-3-3547-5298

* Present address: Department of Pathology, JR Tokyo General Hospital, Tokyo, Japan
** Present address: Department of Structural Biology, Graduate School of Pharmaceutical Sciences, Hokkaido University, Hokkaido, Japan
*** Present address: Department of Surgical Pathology, Sapporo Medical University School of Medicine, Sapporo, Japan

background of synovial sarcoma has been extensively studied to predict the behavior of individual tumors. Synovial sarcomas are characterized by a t(X;18)(p11.2;11.2) fusion, representing the fusion of the SYT gene with either SSX1 or SSX2 [5–8]. Data from clinical samples suggested a link between the type of SYT-SSX protein fusion and the potential for epithelial differentiation; the SYT-SSX1 transcript was found in both monophasic and biphasic tumors, whereas almost all tumors with the SYT-SSX2 transcript were monophasic [9–11]. However, these findings have not been confirmed and were inconsistent in other reports [12, 13]. The differentiation lineage of synovial sarcoma is unclear, and in addition to potential clinical relevance, the regulation of epithelial differentiation in these tumors is a biological issue of interest.

Recent comprehensive studies offered a global view of molecular aberrations associated with the malignant spectrum of synovial sarcoma [14, 15]. Global mRNA expression studies using DNA microarrays identified the genes that are involved in the signaling pathways specific to the cellular origin of synovial sarcoma, the genes associated with histological features denoting malignancy, and the genes differentially expressed corresponding to the different histological subtypes and fusion genes [14, 15]. These comprehensive studies improved our understanding of the biology of synovial sarcoma and may lead to the development of practical tumor markers to support individualized therapy. Emerging technologies that examine the overall features of the expressed proteins, namely the proteome, have identified many candidate proteins associated with early diagnosis [16], differential diagnosis [17], prognosis [18, 19], and response to chemotherapy in various diseases [20] but have not been employed in the study of synovial sarcoma until now.

In this report, we performed a proteomics study on synovial sarcoma clinical samples using 2-D DIGE and MS. We found that the expression levels of 29 protein spots had different intensity corresponding to different histological subtypes. These spots included two variants of GST-P1 (glutathione S-transferase P), a protein the high expression of which has been originally reported to be related to epithelial differentiation [21, 22], drug resistance [22–26] and carcinogenesis [23, 27–34] in malignant tumors other than synovial sarcoma. We verified the expression of GST-P1 in 42 synovial sarcoma cases using immunohistochemistry, and found that it was significantly different between the biphasic and monophasic synovial sarcomas. These results establish GST-P1 as a biomarker for synovial sarcoma differentiation into histological subtypes. GST-P1 may play an important role in the potential for epithelial differentiation of synovial sarcoma.

2 Materials and methods

2.1 Patients and clinical information

We examined the tumor tissues of 49 synovial sarcoma patients who underwent surgery or chemotherapy at the National Cancer Center Hospital consecutively from February 1995 to August 2004. Histological features of the tissues were reviewed by three board-certified pathologists (K. S., T. H., and N. T). Diagnosis and classification was based on the WHO classification system for soft-tissue tumors [1], and included the examination of *SYT-SSX1* and *SYT-SSX2* expression. This project was approved by the institutional review board of the National Cancer Center. Frozen tumor tissues were used for the proteomic analysis, and were available in 28 of 49 cases, including 15 monophasic, 9 biphasic, and 4 poorly differentiated synovial sarcomas. Immunohistochemistry was performed on 42 of 49 cases, consisting of 27 monophasic, 12 biphasic, and 3 poorly differentiated synovial sarcomas. The clinical data pertaining to the cases examined are summarized in Table 1 and Supporting Information Table 1.

2.2 Protein expression profiling

The frozen samples were crushed to powder with a Cryo-Press (Microtech Nichion, Chiba, Japan) under cooling with liquid nitrogen. The frozen powder was then treated with urea lysis buffer (6 M urea, 2 M thiourea, 3% CHAPS, 1% Triton X-100). After centrifugation at 15 000 rpm for 30 min, the supernatant was used as the source of cellular proteins for protein expression studies.

The 2-D DIGE was performed as described previously [17, 18, 20, 35]. In brief, the internal control sample was prepared by mixing a portion of all individual samples. Five micrograms each of the internal control sample and of each individual sample were labeled with Cy3 and Cy5 respectively (CyDye DIGE Fluor saturation dye, GE Healthcare Biosciences, Uppsala, Sweden). The differently labeled protein samples were mixed and then separated, by IPG DryStrip gels for the first dimension separation (24-cm length, p*I* range 4–7, GE Healthcare Biosciences) and then by SDS-PAGE for the second dimension separation (EttanDalt II, GE Healthcare Biosciences). The gels were scanned using laser scanners (Tyhoon Trio, GE Healthcare Biosciences) at the appropriate wavelengths (Fig. 1A and Supporting Information Fig. 1). For all spots, the intensity of the Cy5 image was normalized by that of the Cy3 image from the same gel so that gel-to-gel differences were compensated, using the DeCyder image software (GE Healthcare Biosciences). System reproducibility was verified by comparing the protein profiles obtained from three independent separations of the same sample (sample 22, Table 1 and Supporting Information Table 1). Scatter plot analysis revealed that the standardized intensity of more than 96% of the spots ranged within a twofold difference (Fig. 1B). Representative 2-D images with the numbers of the identified spots are shown in Fig. 1A and Supporting Information Fig. 1.

2.3 Data analysis

The protein spots whose intensity was statistically different between the groups examined were identified using the

Table 1. Clinicopathological features of synovial sarcoma samples (28 cases)

Sample no.	Histological subtype	Age	Gender	Primary location	Fusion gene
1	Monophasic	60	M	Forearm	SYT/SSX2
2	Monophasic	29	M	Shoulder	SYT/SSX1
3	Monophasic	37	M	Shoulder	SYT/SSX1
4	Monophasic	21	M	Knee	SYT/SSX1
5	Monophasic	33	F	Foot	SYT/SSX2
6	Monophasic	17	M	Neck	not detect
7	Monophasic	57	F	Knee	SYT/SSX1
8	Monophasic	30	F	Thigh	SYT/SSX1
9	Monophasic	14	M	Foot	SYT/SSX1
10	Monophasic	26	M	Lower leg	SYT/SSX2
11	Monophasic	41	M	Upper arm	SYT/SSX1
12	Monophasic	40	M	Lower leg	SYT/SSX1
13	Monophasic	52	M	Hand	SYT/SSX1
14	Monophasic	56	F	Retroperitoneum	SYT/SSX1
15	Monophasic	17	F	Lower leg	SYT/SSX2
16	Biphasic	41	F	Thigh	SYT/SSX1
17	Biphasic	41	F	Foot	SYT/SSX1
18	Biphasic	51	M	Hand	SYT/SSX1
19	Biphasic	61	F	Thigh	SYT/SSX1
20	Biphasic	10	F	Elbow	SYT/SSX2
21	Biphasic	27	F	Abdominal wall	not detect
22	Biphasic	33	F	Inguen	SYT/SSX1
23	Biphasic	24	M	Elbow	not detect
24	Biphasic	49	F	Foot	SYT/SSX1
25	Poor	17	F	Thigh	SYT/SSX2
26	Poor	19	F	Thigh	SYT/SSX2
27	Poor	54	M	Inguen	SYT/SSX1
28	Poor	47	F	Thigh	SYT/SSX1

Wilcoxon test (statistical significance was set at $p < 0.01$). Hierarchical clustering, PCA, correlation matrix studies and spot ranking were performed using the Expressionist software (Genedata, Basel, Switzerland).

2.4 Protein identification by MS

Proteins corresponding to the spots of interest were identified by MS according to our previous report [17, 18, 20, 35]. The Cy5-labeled proteins separated by 2-D PAGE were recovered in gel plugs and digested with modified trypsin (Promega, Madison, WI). The trypsin digests were subjected to a Finnigan LTQ linear IT mass spectrometer (Thermo Electron, San Jose, CA) equipped with a nano-electrospray ion source (AMR, Tokyo, Japan). The MASCOT software (version 2.1, Matrix Science, London, UK) was used to search for the mass of the peptide ion peaks against the Swiss-Prot database (*Homo sapiens*, 12 867 sequences in Sprot_47.8 fasta file). A MASCOT score of 35 or more was considered as indicating positive protein identification. When multiple proteins were identified in a single spot, the proteins with the highest number of peptides were considered as those corresponding to the spot.

2.5 Western blotting and immunohistochemistry

Protein samples were separated by SDS-PAGE and subsequently blotted on an NC membrane. The membrane was incubated with a rabbit polyclonal antibody against GST-P1 (1:1000 dilution, MBL international corporation, Woburn, MA), and then HRP-conjugated secondary antibody (1:1000 dilution, GE Healthcare Biosciences). GST-P1 was detected using an enhanced chemiluminescence system (GE Healthcare Biosciences) and LA 3000 (Fuji Film, Tokyo, Japan).

GST-P1 expression was examined immunohistochemically using paraffin-embedded tissues. In brief, 4-μm-thick tissue sections were incubated with the antibody against GST-P1 (1:1000 dilution). Immunostaining was performed according to the streptavidin-biotin peroxidase method using the Strept ABC Complex/HRP kit (DAKO, Tokyo, Japan). Three investigators (Y.S., N.T. and K.S) reviewed the sections stained with the anti-GST-P1 antibody in a blinded fashion regarding clinical data (age, sex, anatomic site, and subtypes). The cases were considered as positive when more than 20% of tumor cells were stained.

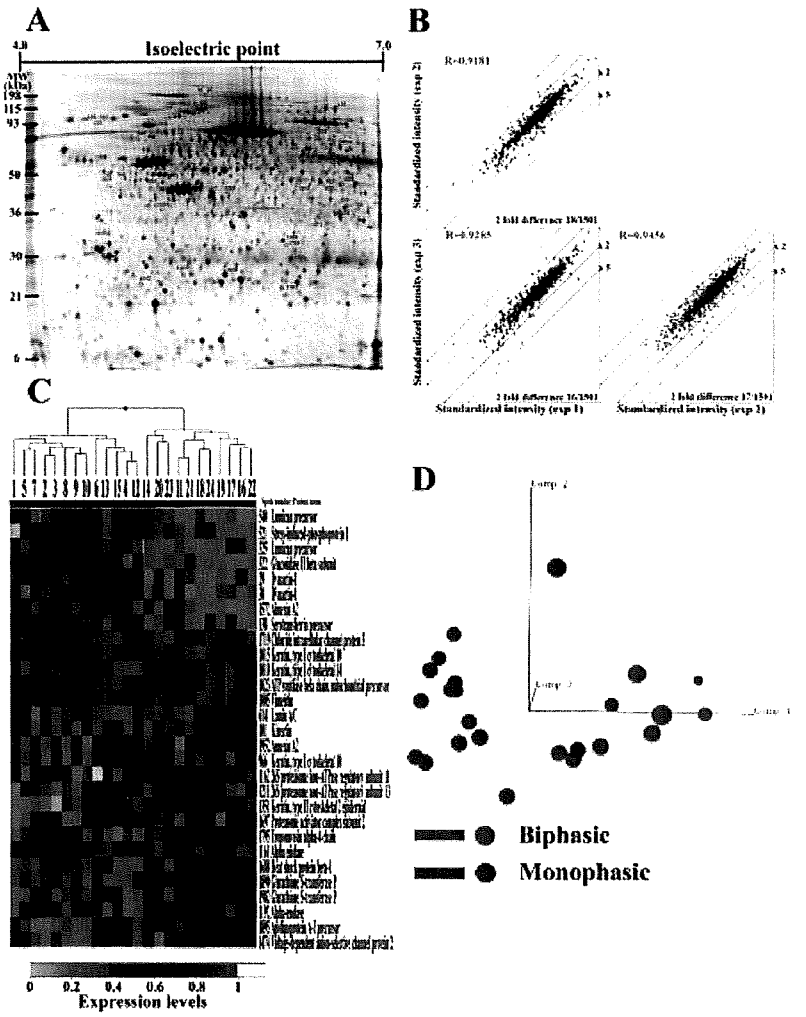

Figure 1. Identification of proteins differentially expressed in the synovial sarcoma subtypes. (A) Representative 2-D gel image of proteins detected in synovial sarcoma tissues. The 29 spots identified in this study are circled and numbered. The spot numbers correspond to those in panel C, Table 2, and Supporting Information Table 2. An enlarged image is shown in Supporting Information Fig. 1. (B) Evaluation of reproducibility of 2-D DIGE by scatter grams. Sample 22 (Table 1 and Supporting Information Table 1) was run in triplicate gels independently. The protein expression profiles were generated by averaging the intensity values acquired in the triplicate gels each time, and the similarity of protein expression profiles was examined by scatter plotting the paired intensities for all spots. (C) Hierarchical clustering of the 24 synovial sarcomas examined based on the intensity of the 29 protein spots. The cases are color-coded as red (biphasic synovial sarcoma) or blue (monophasic synovial sarcoma) as indicated in the panel. The spot numbers and the protein names are shown on the right side. (D) PCA of the 24 synovial sarcoma samples based on the intensity of the 29 protein spots discriminated between the biphasic (red) and monophasic (blue) synovial sarcomas.

2.6 Molecular analysis

We examined the SYT-SSX1 and SYT-SSX2 fusion gene in the 35 of 48 cases for which RNA samples were available. All 35 cases were analyzed by RT-PCR using the primers SYT 5′CAA CAG CAA GAT GCA TAC CA3′, SSX1 5′GGT GCA GTT GTT TCC CAT CG3′ and SSX2 5′GGC ACA GCT CTT TCC CAT CA3′ followed by direct sequencing (Table 1 and Supporting Information Table 1) [9, 13].

2.7 Statistical analysis

Inter-group differences in the age, gender, site, histological subtype, size, depth, MIB-1 index, grade, stage and fusion status between the cases with or without GST-P1 expression were evaluated using the Fisher's exact test or χ^2 test. Statistical analyses were performed using the SPSS statistical package (SPSS, Chicago, IL).

3 Results

We compared the protein expression profiles of 15 monophasic with 9 biphasic synovial sarcomas using 2-D DIGE. In order to decrease irrelevant expression data, we selected the protein spots (1573 in total) that appeared in at least 75% of the images of the Cy3-labeled internal control sample. Although the monophasic type and biphasic subtype cases were not classified into their respective groups based on their overall protein expression profiles (data not shown), 29 protein spots had significantly different intensity between the two groups ($p < 0.01$). The localization of the 29 spots on the 2-D image is demonstrated in Fig. 1A (an enlarged image is shown in Supporting Information Fig. 1). Hierarchical clustering and PCA correctly grouped most cases into the monophasic or the biphasic type based on the intensity of the 29 selected spots (Figs. 1C and D, Supporting Information Figs. 2 and 3). The MS protein identification revealed that

the 29 protein spots corresponded to 24 distinct gene products (Fig. 1C and Supporting Information Fig. 2; Table 2 and Supporting Information Table 2). The results of the protein identification and functional classification are demonstrated in Table 2.

Two of the 29 protein spots were identified as corresponding to GST-P1. We employed SDS-PAGE/Western blotting to further examine the relationship of GST-P1 expression with the histological features of synovial sarcoma and showed that GST-P1 expression was higher in the biphasic compared with the monophasic synovial sarcomas (p <0.0001). The relative protein amounts measured by 2-D DIGE and Western blotting highly correlated with the histological subtype classification for both protein spots (r = 0.680 and 0.722, respectively) (Fig. 2).

The immunohistochemical study of GST-P1 expression in 42 synovial sarcomas revealed a strong correlation between GST-P1 expression and the histological subtype (p = 0.0002, Table 3). Positive expression of GST-P1 was observed in 10 of 12 biphasic cases (83.3%), in 4 of 27 monophasic cases (14.8%) and in 1 of 3 poorly differentiated cases (Table 3 and Supporting Information Table 1). GST-P1 expression was almost exclusively observed in the epithelial component of the biphasic cases, in which it was localized in the membrane and cytoplasm, while most monophasic (spindle cell) cases and the spindle component of the biphasic cases were GST-P1 negative (Fig. 3). When the two main subtypes were compared, the sensitivity and specificity of GST-P1 expression in the biphasic synovial sarcoma was 83.3% and 85.2% respectively (p <0.0001, Supporting Information Table 3). We observed no significant correlation between GST-P1 expression and other clinicopathological parameters examined, including age, gender, and fusion gene status (Table 3). GST-P1 expression had higher power to discriminate between the histological subtypes than the fusion gene status (Supporting Information Table 3). No significant differences were observed (data not shown) when the 2-D

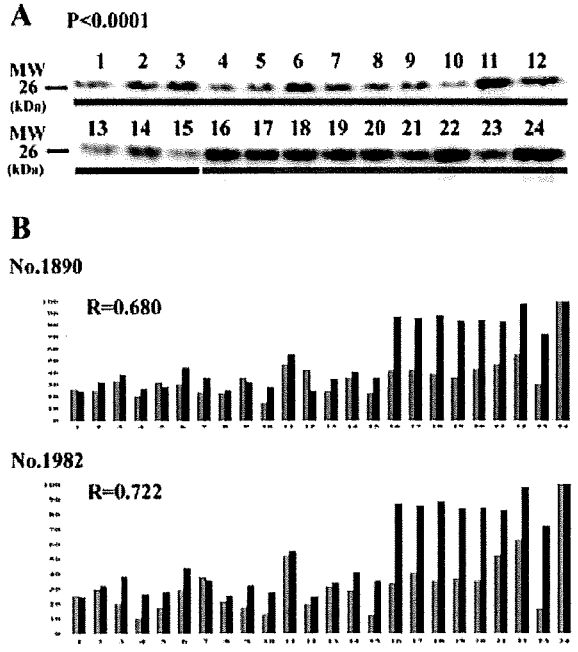

Figure 2. Validation of the differential expression of GST-P1 in the synovial sarcoma subtypes. Biphasic synovial sarcomas (cases 1 to 15) expressed GST-P1 at significantly higher levels than monophasic synovial sarcomas (cases 16 to 24). Case numbers correspond to those in Fig. 1. (A) Western blotting (Mann-Whitney's test p <0.0001). (B) The bar plots demonstrate the GST-P1 expression levels of the two GST-P1 spots (No. 1890 and No. 1982) as detected by 2-D DIGE (grey bars) and Western blotting (black bars) in the 25 synovial sarcoma samples examined. The expression levels detected by 2-D DIGE correlated highly with the ones detected by Western blotting (R = 0.680 for No. 1890 and R = 0.722 for No. 1982).

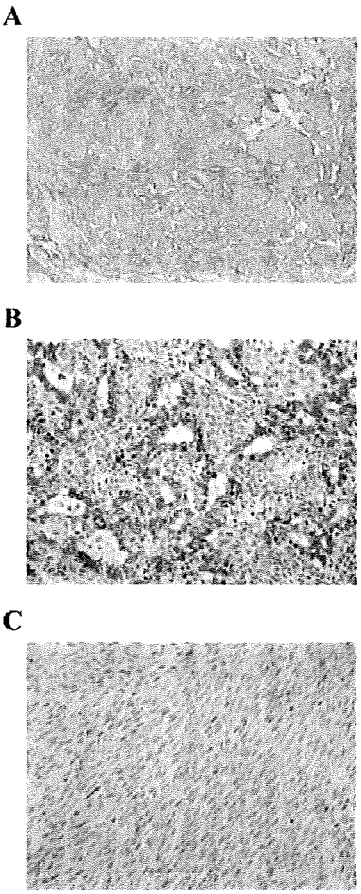

Figure 3. Immunohistochemical expression of GST-P1. (A) GST-P1 was overexpressed in the biphasic synovial sarcoma shown. (B) High-power view of a biphasic synovial sarcoma. GST-P1 expression was almost exclusively observed in the epithelial component, in which it was localized in the membrane and cytoplasm, while the spindle component was GST-P1 negative. (C) GST-P1 was not expressed in the monophasic synovial sarcoma shown.

Table 2. A list of identified proteins

Spot No[a]	Accession No[b]	Identified protein[b]	Wilcoxon test *p* value	Fold difference ratio of means (small intestine/ stomach)	pI (obs)[c]	pI[d]	MW (obs) (kDa)[c]	MW (kDa)[d]	Protein score[e]	Peptide matches	Sequence coverage (%)	Symbol[b]	Function[d]
29	Q14203	Dynactin-1	5.656E-03	1.472	5.46	5.61	198.0	141.7	101	2	1.7	DYNA_HUMAN	Protein binding
30	Q14203	Dynactin-1	9.693E-03	1.405	5.50	5.61	198.0	141.7	128	3	2.4	DYNA_HUMAN	Protein binding
101	Q86UP2	Kinectin	5.485E-04	1.658	5.41	5.52	142.7	156.179	419	8	7.5	KTN1_HUMAN	Vesicle motility
138	P02787	Serotransferrin precursor	8.296E-03	1.907	6.61	6.81	115.0	77.1	135	3	4.4	TRFE_HUMAN	Iron binding transport proteins
322	P14314	Glucosidase II beta subunit precursor	2.896E-03	3.131	4.63	4.34	96.1	59.3	224	5	9.1	GLU2B_HUMAN	Protein kinase cascade
325	P51884	Lumican precursor	7.740E-04	4.177	4.59	6.16	96.1	38.4	63	1	3.3	LUM_HUMAN	Collagen binding
521	P31948	Stress-induced-phosphoprotein 1	1.622E-03	2.291	6.45	6.4	85.5	62.599	230	6	8.8	STIP1_HUMAN	Association of the molecular chaperones
540	P51884	Lumican precursor	5.424E-03	1.410	4.93	6.16	81.8	38.4	68	2	5.9	LUM_HUMAN	Collagen binding
614	P02545	Lamin A/C	4.350E-03	1.556	6.64	6.57	79.9	74.1	947	25	25.3	LAMA_HUMAN	Protein binding
966	P13645	Keratin, type I cytoskeletal 10	7.373E-04	1.434	4.80	5.13	55.6	59.5	702	11	19.1	K1C10_HUMAN	Structural constituent of epidermis
1005	P08670	Vimentin	8.125E-03	2.366	5.16	5.06	50.0	53.5	274	5	10.5	VIME_HUMAN	Protein binding
1010	P02533	Keratin, type I cytoskeletal 14	1.666E-03	1.648	5.11	5.09	50.0	51.5	233	5	8.9	K1C14_HUMAN	Structural constituent of epidermis
1015	P13645	Keratin, type I cytoskeletal 10	2.146E-03	3.491	4.70	5.13	50.0	59.5	438	6	10.6	K1C10_HUMAN	Structural constituent of epidermis
1023	P06576	ATP synthase beta chain, mitochondrial precursor	6.712E-03	1.764	5.07	5.26	50.0	56.6	531	13	21.6	ATPB_HUMAN	Hydrogen ion transporting ATPase activity
1161	P26641	Elongation factor 1-gamma	8.255E-03	2.751	6.64	6.27	46.9	50.0	168	3	5	EF1G_HUMAN	Translation elongation factor activity
1162	O00231	26S proteasome non-ATPase regulatory subunit 11	6.712E-03	1.294	6.30	6.09	47.7	47.3	282	5	10	PSD11_HUMAN	Protein binding
1192	P06733	Alpha-enolase	9.696E-03	1.295	6.57	7.01	47.7	47.139	274	5	13.8	ENOA_HUMAN	Transcription corepressor activity
1211	Q9UNM6	26S proteasome non-ATPase regulatory subunit 13	9.558E-03	1.671	5.70	5.53	43.8	42.891	338	7	14.9	PSD13_HUMAN	Protein binding
1351	P35908	Keratin, type II cytoskeletal 2 epidermal	4.350E-03	1.454	5.09	8.07	43.0	65.9	377	6	11.3	K22E_HUMAN	Structural constituent of epidermis
1474	P45880	Voltage-dependent anion-selective channel protein 2	6.712E-03	1.299	6.59	6.32	35.7	38.1	251	4	14.7	VDAC2_HUMAN	Voltage-gated anion channel activity
1572	P07355	Annexin A2	2.286E-03	1.551	6.45	7.56	35.1	38.5	128	3	9.5	ANXA2_HUMAN	Phospholipase inhibitor activity

Table 2. Continued

Spot No[a]	Accession No[b]	Identified protein[b]	Wilcoxon test *p* value	Fold difference ratio of means (small intestine/ stomach)	p*I* (obs)[c]	p*I*[d]	MW (obs) (kDa)[c]	MW (kDa)[d]	Protein score[e]	Peptide matches	Sequence coverage (%)	Symbol[b]	Function[d]
1688	P04792	Heat shock protein beta-1	2.737E-03	1.757	6.18	5.98	32.4	22.768	421	11	46.3	HSPB1_HUMAN	Cytoskeleton
1697	Q9UL46	Proteasome activator complex subunit 2	5.424E-03	1.299	4.59	5.44	31.2	27.2	268	4	16.4	PSME2_HUMAN	Ubiquitin-protein
1719	O95833	Chloride intracellular channel protein 3	3.465E-03	2.634	6.20	5.99	31.8	26.6	82	2	8.9	CLIC3_HUMAN	Chloride channel activity
1795	P67936	Tropomyosin alpha-4 chain	5.424E-03	1.420	6.23	4.67	29.5	28.504	594	13	33.1	TPM4_HUMAN	Structural constituent of muscle
1890	P09211	Glutathione S-transferase P	2.146E-03	1.642	5.66	5.44	26.2	23.2	136	3	10.5	GSTP1_HUMAN	Protein binding
1895	P02647	Apolipoprotein A-I precursor	4.054E-04	1.288	5.30	5.56	25.7	30.8	717	22	50.9	APOA1_HUMAN	Identical protein binding
1952	P07355	Annexin A2	2.048E-03	1.443	4.96	7.56	23.8	38.5	162	3	9.5	ANXA2_HUMAN	Phospholipase inhibitor activity
1982	P09211	Glutathione S-transferase P	5.424E-03	1.859	6.16	5.44	22.9	23.2	178	4	20.1	GSTP1_HUMAN	Protein binding

a) Spot numbers refer to those in Fig. 1A and Supporting Information Fig. 1.
b) Accession numbers of proteins were derived from Swiss-Prot and NCBI nonredundant databases.
c) Observed p*I* and molecular weight calculated according to location on the 2-D gel.
d) Theoretical p*I* and molecular weight obtained from Swiss-Prot and the ExPASy database (http://au.expasy.org).
e) MASCOT score for the identified proteins based on the peptide ions score ($p < 0.05$) (http://www.matrixscience.com).

Table 3. The relationship between clinico-pathological parameters and GST-p1 expression

Variable	Number of cases	GST-P1 positive (number of cases)	GST-P1 negative (number of cases)	Correlation (GST-P1) χ^2 (p value)
Age				
<40	22	6 (27.27%)	16 (72.73%)	0.2311
40<	20	9 (45.00%)	11 (55.00%)	
Sex				
F	23	10 (43.48%)	13 (56.52%)	0.2479
M	19	5 (26.32%)	14 (73.68%)	
Site				
Trunk	10	3 (30.00%)	7 (70.00%)	0.6657
Extremity	32	12 (37.50%)	20 (62.50%)	
Histology subtype				
Monophasic	27	4 (14.81%)	23 (85.19%)	0.0002
Biphasic	12	10 (83.33%)	2 (16.67%)	
Poor	3	1 (33.33%)	2 (66.67%)	
Fusion				
SYT/SSX1	21	7 (33.33%)	14 (66.67%)	0.264
SYT/SSX2	7	4 (57.14%)	3 (42.86%)	
GST-P1				
Positive	15	–	–	–
Negative	27	–	–	

DIGE data between the monophasic and poorly differentiated synovial sarcomas, biphasic and poorly differentiated sarcomas, or SYT- SSX1 and –SSX2 positive synovial sarcomas were compared.

4 Discussion

The development of a biomarker of histological differentiation of synovial sarcoma has been demanded in order to improve the effectiveness of its management. Global genomic and transcriptomic expression studies conducted to this aim resulted in the identification of EFL3, ERBB2, IGFBP2, heterogeneous nuclear ribonucleoprotein L and hypothetical protein FLJ11273 as such biomarkers [14, 15]. Although these comprehensive studies are expected to further increase our understanding of the biology of synovial sarcoma, they are yet to lead to the development of histological biomarkers that would be of value in a clinical setting. Proteomic studies have a unique advantage over other omics studies, in that the proteome is a functional translation of genome, directly regulating cell phenotypes, and thus is a rich source of potential biomarkers. With this notion, we established a gel-based proteomics system for use in cancer research [17, 18, 20, 35, 36] and applied it to the proteomic study of synovial sarcoma presented here. This is the first report of the use of a proteomic approach to develop histological biomarkers of synovial sarcoma.

Synovial sarcoma is characterized by a translocation between the SYT gene and transcriptional factors [1–4]. The SYT/SSX fusion protein has an altered transcriptional activity and modulates the expression of a number of downstream target genes [37]. In a number of studies, the SYT-SSX1 fusion protein has been reported to be frequently observed in the biphasic subtype of synovial sarcoma, unlike the SYT-SSX2 protein [9–11], while, in contrast, Takenaka *et al* [12, 13]. reported that the status of these fusion genes did not correlate significantly with classification into histological subtypes. Our findings are in agreement with the latter, in that significant correlation between histological subtype classification (monophasic or biphasic) with SYT-SSX fusion type status (-SSX1 or -SSX2) was not observed (p = 0.329, Supporting Information Tables 1 and 3).

Employing proteomics tools, we identified 29 protein variants corresponding to 24 distinct gene products that grouped the synovial sarcoma cases examined according to their histological subtypes (Figs. 1C and D). These included proteins involved in cytoskeletal organization, transcription/translation, protein/collagen binding, and ion transport, as well as structural constituents of the epidermis (Table 2). These findings suggest that the 29 selected variants may induce a large number of functional differences between the histological subtypes of synovial sarcoma. The discriminat-

ing power of this set of proteins may also be useful in the development of practical diagnostic tools in a clinical setting.

Keratin isoforms have been previously proposed as histological markers of biphasic synovial sarcoma [38, 39]. Consistent with these reports, in our analysis, the 29 selected proteins also included keratin isoforms and the expression of keratins 2, 10 and 14 was significantly higher in biphasic synovial sarcoma. We examined the expression of keratin isoforms by Western blotting (Supporting Information Fig. 4). The expression level of keratin isoforms tended to be higher in biphasic type than in monophasic type, suggesting that the sample sets used in this study could be considered as a representative sample set of synovial sarcomas. However, as any single keratins could not perfectly distinguish these histological types, biomarkers that are more specific are required for differential diagnosis.

Two variants of GST-P1 were included in the 29 upregulated proteins. The association of GST-P1 expression with synovial sarcoma has not been previously reported. GST-P1 was originally reported to be a protein highly expressed in the cytoplasm, with a function of protein binding associated with CNS development [23, 30, 31, 40]. GST-P1 has also been reported to be associated with epithelial differentiation [21, 22], drug resistance [23–26], a pre-neoplastic tumor marker [41] and carcinogenesis in breast [29, 31], colon [30, 32], head and neck [42], lung [42], liver cancer [33, 43], and leukemia [28]. It is remarkable that GST-P1 associated with epithelial differentiation [21, 22], and more dominantly observed in the epithelial component of synovial sarcoma, mesenchymal origin, in this study. Activation of GST-P1 contributes to resistance to melphalan [23, 24], doxorubicin [23, 25] and cisplatinum [23, 26], suggesting the possibility of GST-P1 in a clinical use. Although the correlation between GST-P1 and histological subtypes was obvious in our study, the functional contribution of GST-P1 to the histological differentiation is not clear. As GST-P1 was correlated with CNS development [23, 30, 31, 40] and histological differentiation [21, 22], it may have multifunctional properties. With further understanding of the differentiation lineage of synovial sarcoma by clinical observations, the functional properties of GST-P1 in histological differentiation may be clarified. GST-P1 was not identified in previous genome and transcriptome studies as being involved in synovial sarcoma pathogenesis [14, 15], suggesting that the study of the proteome is able to reveal unique molecular aspects of synovial sarcoma.

GST-P1 was identified in two protein spots, No. 1890 and No. 1982. These two protein spots had different p*I*s and molecular weights, the degree of which may not be simply attributable to phosphorylation and glycosylation. The other mechanisms to generate protein variants, such as alternative splicing and protein cleavage, may be responsible to the different electrophoretic mobilities of these protein spots. There are many examples of alternative splicing, resulting in the protein variants with different molecular weight [44]. Chignard *et al.* [45] reported the cleaved endoplasmic reticulum protein as a novel biomarker candidate in hepatocellular carcinoma. As the protein variants often have unique functionalities and clinical utilities, further investigations on those two protein spots for GST-P1 will be interesting.

The proteins that were observed in two or more spots included keratin 10, dynactin-1, the lumican precursor, and annexin 2. As mentioned earlier, keratin 10 was expressed in biphasic synovial sarcoma cases, while dynactin-1 and the lumican precursor were expressed in monophasic cases, and annexin 2 was expressed in both subtypes. Keratin 10 has been identified as being a structural constituent of the epidermis and as promoting the epidermis differentiation of squamous carcinomas [46–49]. Dynactin-1 facilitates mitosis and nervous system development [50–55]. The lumican precursor is an extracellular matrix structural constituent and its activation contributes to collagen binding [56–60]. Finally, activation of annexin 2 promotes the formation of a calcium-regulated membrane-binding protein whose affinity for calcium is greatly enhanced by anionic phospholipids [61]. The PTM, including phosphorylation, glycosylation and degradation may affect the p*I* and molecular weight of proteins, changing the electrophoretic mobility of proteins. The protein spots from same protein may have different functions in the cells, as they have different physical characters. In addition to examining diagnostic utilities of each protein spot, the functional studies will be of great interest.

Our results suggest that GST-P1 may be a novel histological biomarker for patients with synovial sarcoma. We demonstrated that GST-P1 expression can be examined by SDS-PAGE/Western blotting and immunohistochemistry. Moreover, using a large-scale sample set and immunohistochemistry, we showed that the expression pattern of GST-P1 differs significantly between biphasic and monophasic synovial sarcomas and can therefore be used to differentiate them (Table 3 and Supporting Information Table 3).

There was no significant correlation between GST-P1 expression and the other clinicopathological parameters examined (Table 3), or between GST-P1 expression and fusion gene status (Table 3). These findings establish GST-P1 as a novel histological marker for synovial sarcoma subtypes, and suggest that GST-P1 may play an important role in the epithelial differentiation of synovial sarcoma.

In conclusion, we identified a possible correlation of 29 protein variants corresponding to 24 distinct gene products with differentiation into histological subtypes in synovial sarcoma. Furthermore, we validated GST-P1 expression using a specific antibody and found that GST-P1 distinguished biphasic from monophasic synovial sarcoma, suggesting its utility in the classification of synovial sarcoma into histological subtypes. Assessment of the diagnostic value of the combined use of GST-P1 and the other 23 proteins, as well as a more extensive validation of GST-P1 expression on additional samples are now underway in our laboratory.

This work was supported by a grant from the Ministry of Health, Labor and Welfare and by the Program for Promotion of Fundamental Studies in Health Sciences of the National Institute of Biomedical Innovation of Japan, a grant-in-aid for Young Scientists (start-up) No. 20890218 from the Japan Society for the Promotion of Science and the International Society of Orthopaedic Surgery and Traumatology. The excellent technical support provided by Kano Nishiyama and Yukiko Fujie in electrophoresis is greatly appreciated.

The authors have declared no conflict of interest.

5 References

[1] Fletcher, C., Unni, K., Mertens, F., *Pathology and Genetics Tumours of Soft Tissue and Bone.* IARCP Press, Lyon, France 2002, pp. 200-204.

[2] Lewis, J. J., Antonescu, C. R., Leung, D. H., Blumberg, D. *et al.*, Synovial sarcoma: a multivariate analysis of prognostic factors in 112 patients with primary localized tumors of the extremity. *J. Clin. Oncol.* 2000, *18*, 2087–2094.

[3] Spillane, A. J., A'Hern, R., Judson, I. R., Fisher, C., Thomas, J. M., Synovial sarcoma: a clinicopathologic, staging, and prognostic assessment. *J. Clin. Oncol.* 2000 *18* 3794–3803.

[4] Trassard, M., Le Doussal, V., Hacene, K., Terrier, P *et al.*, Prognostic factors in localized primary synovial sarcoma: a multicenter study of 128 adult patients. *J. Clin. Oncol.* 2001, *19*, 525–534.

[5] Clark, J., Rocques, P. J., Crew, A. J., Gill, S. *et al.*, Identification of novel genes, SYT and SSX, involved in the t(X;18)(p11.2;q11.2) translocation found in human synovial sarcoma. *Nat. Genet.* 1994, *7*, 502–508.

[6] Skytting, B., Nilsson, G., Brodin, B., Xie, Y. *et al.*, A novel fusion gene, SYT-SSX4, in synovial sarcoma. *J. Natl. Cancer Inst.* 1999, *91*, 974–975.

[7] Nagai, M., Tanaka, S., Tsuda, M., Endo, S. *et al.*, Analysis of transforming activity of human synovial sarcoma-associated chimeric protein SYT-SSX1 bound to chromatin remodeling factor hBRM/hSNF2 alpha. *Proc. Natl. Acad. Sci. USA* 2001, *98*, 3843–3848.

[8] dos Santos, N. R., de Bruijn, D. R., van Kessel, A. G., Molecular mechanisms underlying human synovial sarcoma development. *Genes Chromosomes Cancer* 2001, *30*, 1–14.

[9] Kawai, A., Woodruff, J., Healey, J. H., Brennan, M. F. *et al.*, SYT-SSX gene fusion as a determinant of morphology and prognosis in synovial sarcoma. *N. Engl. J. Med.* 1998, *338*, 153–160.

[10] Antonescu, C. R., Kawai, A., Leung, D. H., Lonardo, F. *et al.*, Strong association of SYT-SSX fusion type and morphologic epithelial differentiation in synovial sarcoma. *Diagn. Mol. Pathol.* 2000, *9*, 1–8.

[11] Ladanyi, M., Correlates of SYT-SSX fusion type in synovial sarcoma: getting more complex but also more interesting? *J. Clin. Oncol.* 2005, *23*, 3638–3639; author reply 3639–3640.

[12] Guillou, L., Benhattar, J., Bonichon, F., Gallagher, G. *et al.*, Histologic grade, but not SYT-SSX fusion type, is an important prognostic factor in patients with synovial sarcoma: a multicenter, retrospective analysis. *J. Clin. Oncol.* 2004, *22*, 4040–4050.

[13] Takenaka, S., Ueda, T., Naka, N., Araki, N. *et al.*, Prognostic implication of SYT-SSX fusion type in synovial sarcoma: a multi-institutional retrospective analysis in Japan. *Oncol. Rep.* 2008, *19*, 467–476.

[14] Allander, S. V., Illei, P. B., Chen, Y., Antonescu, C. R. *et al.*, Expression profiling of synovial sarcoma by cDNA microarrays: association of ERBB2, IGFBP2, and ELF3 with epithelial differentiation. *Am. J. Pathol.* 2002, *161*, 1587–1595.

[15] Nagayama, S., Katagiri, T., Tsunoda, T., Hosaka, T. *et al.*, Genome-wide analysis of gene expression in synovial sarcomas using a cDNA microarray. *Cancer Res.* 2002, *62*, 5859–5866.

[16] Petricoin, E. F., Ardekani, A. M., Hitt, B. A., Levine, P. J. *et al.*, Use of proteomic patterns in serum to identify ovarian cancer. *Lancet* 2002, *359*, 572–577.

[17] Suehara, Y., Kondo, T., Fujii, K., Hasegawa, T. *et al.*, Proteomic signatures corresponding to histological classification and grading of soft-tissue sarcomas. *Proteomics* 2006, *6*, 4402–4409.

[18] Suehara, Y., Kondo, T., Seki, K., Shibata, T. *et al.*, Pfetin as a prognostic biomarker of gastrointestinal stromal tumors revealed by proteomics. *Clin. Cancer Res.* 2008, *14*, 1707–1717.

[19] Chen, G., Gharib, T. G., Wang, H., Huang, C. C. *et al.*, Protein profiles associated with survival in lung adenocarcinoma. *Proc. Natl. Acad. Sci. USA* 2003, *100*, 13537–13542.

[20] Okano, T., Kondo, T., Fujii, K., Nishimura, T. *et al.*, Proteomic signature corresponding to the response to gefitinib (Iressa, ZD1839), an epidermal growth factor receptor tyrosine kinase inhibitor in lung adenocarcinoma. *Clin. Cancer Res.* 2007, *13*, 799–805.

[21] Shimizu, K., Toriyama, F., Yoshida, H., The expression of placental-type glutathione S-transferase (GST-pi) in human cutaneous squamous cell carcinoma and normal human skin. *Virchows Arch.* 1995 *425*, 589–592.

[22] Konohana, A., Konohana, I., Schroeder, W. T., O'Brien, W. R. *et al.*, Placental glutathione-S-transferase-pi mRNA is abundantly expressed in human skin. *J. Invest. Dermatol.* 1990, *95*, 119–126.

[23] Moscow, J. A., Townsend, A. J., Cowan, K. H., Elevation of pi class glutathione S-transferase activity in human breast cancer cells by transfection of the GST pi gene and its effect on sensitivity to toxins. *Mol. Pharmacol.* 1989, *36*, 22–28.

[24] Manoharan, T. H., Puchalski, R. B., Burgess, J. A., Pickett, C. B., Fahl, W. E., Promoter-glutathione S-transferase Ya cDNA hybrid genes. Expression and conferred resistance to an alkylating molecule in mammalian cells. *J. Biol. Chem.* 1987 *262*, 3739–3745.

[25] Morrow, C. S., Cowan, K. H., Goldsmith, M. E., Structure of the human genomic glutathione S-transferase-pi gene. *Gene* 1989 *75*, 3–11.

[26] Teicher, B. A., Holden, S. A., Kelley, M. J., Shea, T. C. *et al.*, Characterization of a human squamous carcinoma cell line resistant to cis-diamminedichloroplatinum(II). *Cancer Res.* 1987 *47*, 388–393.

[27] Shea, T. C., Kelley, S. L., Henner, W. D., Identification of an anionic form of glutathione transferase present in many hu-

man tumors and human tumor cell lines. *Cancer Res.* 1988, *48*, 527–533.

[28] Allan, J. M., Wild, C. P., Rollinson, S., Willett, E. V. *et al.*, Polymorphism in glutathione S-transferase P1 is associated with susceptibility to chemotherapy-induced leukemia. *Proc. Natl. Acad. Sci. USA* 2001, *98*, 11592–11597.

[29] Arai, T., Miyoshi, Y., Kim, S. J., Taguchi, T. *et al.*, Association of GSTP1 CpG islands hypermethylation with poor prognosis in human breast cancers. *Breast Cancer Res. Treat.* 2006 *100*, 169–176.

[30] Kano, T., Sakai, M., Muramatsu, M., Structure and expression of a human class pi glutathione S-transferase messenger RNA. *Cancer Res.* 1987 *47*, 5626–5630.

[31] Moscow, J. A., Townsend, A. J., Goldsmith, M. E., Whang-Peng, J. *et al.*, Isolation of the human anionic glutathione S-transferase cDNA and the relation of its gene expression to estrogen-receptor content in primary breast cancer. *Proc. Natl. Acad. Sci. USA* 1988, *85*, 6518–6522.

[32] Kodate, C., Fukushi, A., Narita, T., Kudo, H. *et al.*, Human placental form of glutathione S-transferase (GST-pi) as a new immunohistochemical marker for human colonic carcinoma. *Jpn. J. Cancer Res.* 1986, *77*, 226–229.

[33] Li, Y. C., Seyama, T., Godwin, A. K., Winokur, T. S. *et al.*, MTrasT24, a metallothionein-ras fusion gene, modulates expression in cultured rat liver cells of two genes associated with *in vivo* liver cancer. *Proc. Natl. Acad. Sci. USA* 1988, *85*, 344–348.

[34] Buller, A. L., Clapper, M. L., Tew, K. D., Glutathione S-transferases in nitrogen mustard-resistant and -sensitive cell lines. *Mol. Pharmacol.* 1987, *31*, 575–578.

[35] Kondo, T.,Hirohashi, S., Application of highly sensitive fluorescent dyes (CyDye DIGE Fluor saturation dyes) to laser microdissection and two-dimensional difference gel electrophoresis (2D-DIGE) for cancer proteomics. *Nat. Protoc.* 2006, *1*, 2940–2956.

[36] Klose, J., Nock, C., Herrmann, M., Stuhler, K. *et al.*, Genetic analysis of the mouse brain proteome. *Nat. Genet.* 2002, *30*, 385–393.

[37] Xie, Y., Tornkvist, M., Aalto, Y., Nilsson, G. *et al.*, Gene expression profile by blocking the SYT-SSX fusion gene in synovial sarcoma cells. Identification of XRCC4 as a putative SYT-SSX target gene. *Oncogene* 2003, *22*, 7628–7631.

[38] Miettinen, M., Keratin subsets in spindle cell sarcomas. Keratins are widespread but synovial sarcoma contains a distinctive keratin polypeptide pattern and desmoplakins. *Am. J. Pathol.* 1991, *138*, 505–513.

[39] Miettinen, M., Limon, J., Niezabitowski, A., Lasota, J., Patterns of keratin polypeptides in 110 biphasic, monophasic, and poorly differentiated synovial sarcomas. *Virchows Arch.* 2000, *437*, 275–283.

[40] Wanibuchi, H., Wei, M., Karim, M. R., Morimura, K. *et al.*, Existence of no hepatocarcinogenic effect levels of 2-amino-3,8-dimethylimidazo[4,5-f]quinoxaline with or without coadministration with ethanol. *Toxicol. Pathol.* 2006, *34*, 232–236.

[41] Sato, K., Glutathione transferases as markers of preneoplasia and neoplasia. *Adv. Cancer Res.* 1989, *52*, 205–255.

[42] Moscow, J. A., Fairchild, C. R., Madden, M. J., Ransom, D. T. *et al.*, Expression of anionic glutathione-S-transferase and P-glycoprotein genes in human tissues and tumors. *Cancer Res.* 1989, *49*, 1422–1428.

[43] Satoh, K., Kitahara, A., Soma, Y., Inaba, Y. *et al.*, Purification, induction, and distribution of placental glutathione transferase: a new marker enzyme for preneoplastic cells in the rat chemical hepatocarcinogenesis. *Proc. Natl. Acad. Sci. USA* 1985, *82*, 3964–3968.

[44] Blencowe, B. J., Alternative splicing: new insights from global analyses. *Cell* 2006, *126*, 37–47.

[45] Chignard, N., Shang, S., Wang, H., Marrero, J. *et al.*, Cleavage of endoplasmic reticulum proteins in hepatocellular carcinoma: Detection of generated fragments in patient sera. *Gastroenterology* 2006, *130*, 2010–2022.

[46] Santos, M., Ballestin, C., Garcia-Martin, R., Jorcano, J. L., Delays in malignant tumor development in transgenic mice by forced epidermal keratin 10 expression in mouse skin carcinomas. *Mol. Carcinog.* 1997, *20*, 3–9.

[47] Ivanyi, D., Ansink, A., Mooi, W. J., de Kraker, N. W., Heintz, A. P., Absence of differentiation-related expression of keratin 10 in early stages of vulvar squamous carcinoma. *Differentiation* 1989, *42*, 124–129.

[48] Ivanyi, D., Ansink, A., Groeneveld, E., Hageman, P. C. *et al.*, New monoclonal antibodies recognizing epidermal differentiation-associated keratins in formalin-fixed, paraffin-embedded tissue. Keratin 10 expression in carcinoma of the vulva. *J. Pathol.* 1989, *159*, 7–12.

[49] Darmon, M. Y., Semat, A., Darmon, M. C., Vasseur, M., Sequence of a cDNA encoding human keratin No 10 selected according to structural homologies of keratins and their tissue-specific expression. *Mol. Biol. Rep.* 1987, *12*, 277–283.

[50] Melloni, R. H., Jr., Tokito, M. K., Holzbaur, E. L., Expression of the p150Glued component of the dynactin complex in developing and adult rat brain. *J. Comp. Neurol.* 1995, *357*, 15–24.

[51] Murphey, R. K., Caruccio, P. C., Getzinger, M., Westgate, P. J., Phillis, R. W., Dynein-dynactin function and sensory axon growth during Drosophila metamorphosis: A role for retrograde motors. *Dev. Biol.* 1999, *209*, 86–97.

[52] Eaton, B. A., Fetter, R. D., Davis, G. W., Dynactin is necessary for synapse stabilization. *Neuron* 2002, *34*, 729–741.

[53] Levy, J. R., Sumner, C. J., Caviston, J. P., Tokito, M. K. *et al.*, A motor neuron disease-associated mutation in p150Glued perturbs dynactin function and induces protein aggregation. *J. Cell. Biol.* 2006, *172*, 733–745.

[54] Mikenberg, I., Widera, D., Kaus, A., Kaltschmidt, B., Kaltschmidt, C., Transcription factor NF-kappaB is transported to the nucleus via cytoplasmic dynein/dynactin motor complex in hippocampal neurons. *PLoS ONE* 2007, *2*, e589.

[55] Ateh, D. D., Hussain, I. K., Mustafa, A. H., Price, K. M. *et al.*, Dynein-dynactin complex subunits are differentially localized in brain and spinal cord, with selective involvement in pathological features of neurodegenerative disease. *Neuropathol. Appl. Neurobiol.* 2008, *34*, 88–94.

[56] Sifaki, M., Assouti, M., Nikitovic, D., Krasagakis, K. *et al.*, Lumican, a small leucine-rich proteoglycan substituted with keratan sulfate chains is expressed and secreted by human

